Reynolds-Stress Model Analysis of Turbulent Flow over a Curved Axisymmetric Body

Shin Bae Park,* Myung Kyoon Chung,† and Do Hyung Choi‡
Korea Advanced Institute of Science and Technology, Seoul, Korea

A curvature-dependent Reynolds-stress model (CRSM) is proposed for prediction of complex turbulent flows over curved surfaces. A curvature time scale for the third-order diffusive transport terms in the Reynolds-stress equations is assumed, which is derived from analogy between buoyancy and streamline curvature effects on turbulence. The coefficient of the destruction term in the dissipation equation is also modified by the proposed time scale in order to incorporate the streamline curvature effect on the decay rate of turbulent kinetic energy. The proposed CRSM is applied to a mildly curved axisymmetric body: a spheroid of axis ratio 6:1 for which Reynolds-stress data are available. The results show that the model performs better than the well-established k–ϵ turbulence model. In particular, all the predicted Reynolds-stress components are in very good agreement with experimental data.

Introduction

MODELING of the Reynolds stresses that appear in the Reynolds-averaged Navier-Stokes equations has received considerable attention in recent years for prediction of complex turbulent flows occurring in many engineering applications. As the computing power of modern computers continues to grow and the cost decreases, many practical problems are becoming tractable through solutions of the equations for Reynolds stresses. In such cases, the success of the turbulent-flow prediction depends more on the turbulence model than on the numerical scheme. For example, comparisons made at the 1980–1981 Stanford conference[1] on complex turbulent flows showed that solutions of the Reynolds-averaged Navier-Stokes equations were very much dependent on the turbulence model used.

Most applications of Reynolds-stress models have been made to rather simple geometries. In the present study, however, a Reynolds-stress model is applied to a geometric shape with surface curvature. Development of the turbulence structure is highly sensitive to streamline curvature in the plane of the mean-shear flow.[2] Firstly, Reynolds stresses are reduced by streamline curvature when the angular momentum of a fluid element increases in the direction of the radius of curvature, as in the case of the flow over a convex surface. The opposite is observed on a concave surface. Secondly, the response of turbulence to convex curvature is much more rapid than that to concave curvature. Thirdly, it has been found experimentally that the time response of the third-order correlations to convex streamline curvature is slower than that of the second-order correlations.[2,3] Therefore, for the prediction to be successful, these experimental observations must be taken into account in the modeling of the Reynolds-stress transport equations. However, most previous curvature-correction methods[4–7] do not explicitly include such effects.

Recently, a curvature-dependent k–ϵ turbulence model was proposed by Park and Chung[8] for prediction of turbulent recirculating flow in which the time scale of the third-order diffusive transport terms in the equations for k and ϵ was made a function of the ratio between a curvature time scale and a velocity time scale. They applied their model to several recirculating flows with success. The present study is an extension of this approach to include streamline curvature effects in the Reynolds-stress-model equations. The conventional model coefficients of the diffusive transport terms and the destruction term in the ϵ equation are modified to incorporate the time-scale ratio mentioned above. The performance of the proposed model is tested against the data of Chevray.[9] The results are also compared with the earlier computation of Chen and Patel[10] who used a two-layer k–ϵ turbulence model.

Received June 8, 1989; revision received March 19, 1990; second revision received May 30, 1990; accepted for publication May 31, 1990.

*Graduate Student, Department of Mechanical Engineering.
†Professor, Department of Mechanical Engineering.
‡Professor, Department of Mechanical Engineering. Member AIAA.

Curvature-Dependent Reynolds-Stress Model

The Reynolds-averaged Navier-Stokes equations in Cartesian coordinates for incompressible flow with constant viscosity are

$$\frac{\partial U_i}{\partial x_i} = 0 \tag{1}$$

$$\frac{\mathrm{D}U_i}{\mathrm{D}t} = -\frac{1}{\rho}\frac{\partial \bar{P}}{\partial x_i} + \nu\frac{\partial^2 U_i}{\partial x_l \partial x_l} - \frac{\partial \overline{u_i u_j}}{\partial x_j} \tag{2}$$

Here U_i and u_i are the mean and fluctuating parts of velocity, respectively, $\bar{P}$ the static pressure, ρ the density, ν the kinematic viscosity, and $\overline{u_i u_j}$ the Reynolds-stress tensor. The exact equations governing the Reynolds stresses can be written (Tennekes and Lumley[11]):

$$\frac{\mathrm{D}\overline{u_i u_j}}{\mathrm{D}t} = -\frac{\partial}{\partial x_l}\left[\overline{u_i u_j u_l} + \frac{1}{\rho}\overline{p(\delta_{jl}u_i + \delta_{il}u_j)} - \nu\frac{\partial \overline{u_i u_j}}{\partial x_l}\right] - \left[\overline{u_i u_l}\frac{\partial U_j}{\partial x_l} + \overline{u_j u_l}\frac{\partial U_i}{\partial x_l}\right] - 2\nu\overline{\frac{\partial u_i}{\partial x_l}\frac{\partial u_j}{\partial x_l}} + \frac{1}{\rho}\overline{p\left(\frac{\partial u_i}{\partial x_j} + \frac{\partial u_j}{\partial x_i}\right)} \tag{3}$$

Here the averaged terms with overbars, except $\overline{u_i u_j}$, need to be modeled in order to close the system of equations. Among various closure relations,[12–14] the model by Nobuyuki[14] for the Reynolds-stress tensor appears to be most convenient for the present study:

$$\frac{\mathrm{D}\overline{u_i u_j}}{\mathrm{D}t} = -\frac{\partial}{\partial x_l}\left[\overline{u_i u_j u_l} - \nu\frac{\partial \overline{u_i u_j}}{\partial x_l}\right] + P_{ij} + E_{ij} + R_{ij} + R_{wij} \tag{4}$$

where

$$-\overline{u_iu_ju_l} = C_s\frac{k}{\epsilon}\left(\overline{u_iu_m}\frac{\partial\overline{u_ju_l}}{\partial x_m}+\overline{u_ju_m}\frac{\partial\overline{u_iu_l}}{\partial x_m}+\overline{u_lu_m}\frac{\partial\overline{u_iu_j}}{\partial x_m}\right) \quad (5)$$

$$P_{ij} = \left(\overline{u_ju_l}\frac{\partial U_i}{\partial x_l}+\overline{u_iu_l}\frac{\partial U_j}{\partial x_l}\right) \quad (6)$$

$$E_{ij} = -\frac{\epsilon}{k}\overline{u_iu_j} \quad (7)$$

$$R_{ij} = -C_1^*\frac{\epsilon}{k}\left(\overline{u_iu_j}-\frac{2}{3}\delta_{ij}k\right)-\frac{C_2+8}{11}\left(P_{ij}-\frac{2}{3}\delta_{ij}P\right) - \frac{30C_2-2}{55}k\left(\frac{\partial U_i}{\partial x_j}+\frac{\partial U_j}{\partial x_i}\right)-\frac{8C_2-2}{11}\left(D_{ij}-\frac{2}{3}\delta_{ij}P\right) \quad (8)$$

$$D_{ij} = -\left(\overline{u_iu_l}\frac{\partial U_l}{\partial x_j}+\overline{u_ju_l}\frac{\partial U_l}{\partial x_i}\right) \quad (9)$$

$$P = -\overline{u_lu_m}\frac{\partial U_l}{\partial x_m}, \qquad k = \frac{1}{2}\overline{u_iu_i} \quad (10)$$

and

$$R_{wij} = \left[\alpha\left(P_{ij}-\frac{2}{3}\delta_{ij}P\right)+\beta\left(D_{ij}-\frac{2}{3}\delta_{ij}P\right) + \gamma k\left(\frac{\partial U_i}{\partial x_j}+\frac{\partial U_j}{\partial x_i}\right)\right]f_w \quad (11)$$

The constants in the preceding equations are $C_s = 0.11$, $C_1^* = C_1[1-(1-1/C_1)f_w]$, $C_1 = 1.5$, and $C_2 = 0.4$. The wall damping function f_w is given as $f_w = \exp[-(0.015\,k^{1/2}y/\nu)^4]$, and the coefficients α, β, and γ are 0.45, -0.03, and 0.08, respectively.

In the conventional gradient-transport model for the triple-velocity correlations, $\overline{u_iu_ju_l}$, the velocity time scale $\tau_v = k/\epsilon$ is independent of streamline curvature. But it has been found that these correlations must have a curvature-dependent time scale.[15] Such curvature effect has been modeled by devising a curvature time scale τ_c by analogy between buoyancy and streamline curvature effects on turbulence. Adopting the same modification as in Chung et al.,[15] the model constant C_s for the triple-velocity correlation is replaced by C_s', a function of the time-scale ratio:

$$C_s' = C_s/[1+a(\tau_v/\tau_c)] \quad (12)$$

where $\tau_c = \epsilon/(N_c^2k)$, N_c is the frequency of oscillations of a fluid element displaced radially with reference to streamline curvature, and $a = 0.12$ is a model constant.

As for the dissipation rate of turbulent kinetic energy, the equation suggested by Hanjalic and Launder[13] is used here in the following form:

$$\frac{D\epsilon}{Dt} = -\frac{\partial}{\partial x_l}\left[\overline{\epsilon' u_l}-\nu\frac{\partial\epsilon}{\partial x_l}\right]+C_{\epsilon1}\frac{\epsilon}{k}P-C_{\epsilon2}f_\epsilon\frac{\epsilon\bar{\epsilon}}{k}+\varphi \quad (13)$$

where

$$-\overline{\epsilon' u_l} = C_\epsilon\frac{k}{\epsilon}\overline{u_lu_m}\frac{\partial\epsilon}{\partial x_m} \quad (14)$$

$$\bar{\epsilon} = \epsilon - 2\nu\left(\frac{\partial\sqrt{k}}{\partial x_l}\right)^2 \quad (15)$$

$$f_\epsilon = 1.0-\frac{0.4}{1.8}\exp(-R_\tau^2/36) \quad (16)$$

$$\varphi = C_{\epsilon3}\nu\frac{k}{\epsilon}\overline{u_ju_l}\frac{\partial^2U_i}{\partial x_j\partial x_m}\frac{\partial^2U_i}{\partial x_l\partial x_m} \quad (17)$$

The model constants in the preceding equations are $C_\epsilon = 0.15$, $C_{\epsilon1} = 1.44$, $C_{\epsilon2} = 1.9$, and $C_{\epsilon3} = 2.0$, and $R_\tau = k^2/\nu\epsilon$ is the turbulence Reynolds number. In the wake, where there is no boundary, $C_{\epsilon3}$ is set to zero. To simulate transition from a near-wall sublayer to a fully turbulent wake correctly, the functions f_ϵ, f_w and $\bar{\epsilon}/\epsilon$ need to be modified to increase gradually to unity through the very near wake (see Refs. 10 and 16). Although we recognize this subtlety, we assume that the flow becomes turbulent instantly in the wake and set $f_\epsilon = f_w = 1$ and $\bar{\epsilon} = \epsilon$ at the tail of the body.

The coefficient C_ϵ of the third-order correlation term (14) in the ϵ equation is modified similarly as $\overline{u_iu_ju_l}$ in order to take the streamline curvature effect into account. In other words, C_ϵ is modified as

$$C_\epsilon' = C_\epsilon\left[\frac{1}{1+b(\tau_v/\tau_c)}\right] \quad (18)$$

As the decay rate of turbulent kinetic energy also depends on streamline curvature,[2] it is convenient to represent such effect as:

$$C_{\epsilon2}' = C_{\epsilon2}\left[\frac{1}{1+b(\tau_v/\tau_c)}\right] \quad (19)$$

as was done in Ref. 8. Here, b is a model constant and assumes a value of 0.5.

All of the equations described so far can be summarized in cylindrical polar coordinates (x,r,θ) as

$$\frac{\partial\phi}{\partial t}+U\frac{\partial\phi}{\partial x}+V\frac{\partial\phi}{\partial r} = \frac{\partial}{\partial x}\left(\Gamma_1\frac{\partial\phi}{\partial x}\right)+\frac{1}{r}\frac{\partial}{\partial r}\left(r\Gamma_2\frac{\partial\phi}{\partial r}\right)+S_\phi \quad (20)$$

where ϕ represents one of the transport quantities, i.e., U, V, $\overline{u^2}$, $\overline{v^2}$, $\overline{w^2}$, $\overline{uv}$, or ϵ. The variables in the equation have been made dimensionless in terms of the freestream velocity U_o, the body length L, and density ρ.

Numerical Method and Boundary Conditions

The solution of Eq. (20) is sought in the domain shown in Fig. 1. The solution procedure adopted in the present study is essentially the same as that described in Chen and Patel[16] and is briefly explained below. Computation is performed in body-fitted coordinates (ξ,η) that are generated numerically. Using the expressions for the gradient, divergence, Laplacian, and second-order derivatives (given in Ref. 16), Eq. (20) can be transformed to this computational plane and the resulting equation assumes the following form:

$$A^{11}\phi_{\xi\xi}+A^{22}\phi_{\eta\eta} = D_\phi\phi_l+2A_\phi\phi_\xi+2B_\phi\phi_\eta+S_\phi^T \quad (21)$$

where A^{11}, A^{22} are geometric coefficients; A_ϕ, B_ϕ, D_ϕ the linearized convection coefficients; and S_ϕ^T the source term. Equation (21) is then solved by using the finite-analytic algorithm of Ref. 16.

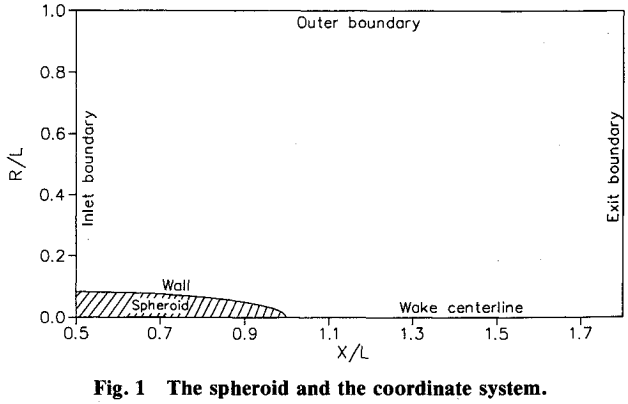

Fig. 1 The spheroid and the coordinate system.

Since the governing equation (20) is elliptic, the boundary conditions need to be prescribed on all boundaries: inlet, exit, outer, wall, and wake centerline (see Fig. 1). A separate boundary-layer calculation was performed from the stagnation point to construct the conditions at the inlet boundary. The finite-difference procedure of Chang and Patel[17] used here gives the inlet profiles of the mean velocity, the Reynolds shear stress $-\overline{uv}$, and the eddy viscosity ν_t. The turbulent kinetic energy k and dissipation ϵ are deduced from the following empirical relationships:

$$k = -\overline{uv}/0.3 \tag{22}$$

$$\epsilon = 0.09\,\frac{k^2}{\nu_t} \tag{23}$$

The normal stresses, $\overline{u^2}$, $\overline{v^2}$, and $\overline{w^2}$ are then obtained by assuming isotropy at the inlet station, and this completes the description of the inlet boundary conditions.

Along the exit boundary, which is placed far downstream of the body, the streamwise derivatives of the dependent variables and pressure are assumed negligible, i.e., $(\partial/\partial\xi) = 0$. The outer boundary is also placed far away (approximately one body length) from the surface where the disturbance due to the body is expected to be small.[10] Therefore, uniform-flow conditions are imposed along this boundary. Symmetry condition is applied at the wake centerline and, since a wall-function approach is used in the analysis, the following near-wall approximations, suggested by Launder et al.,[12] are used for the wall boundary:

$$\overline{u^2} = 5.1\,U_\tau^2, \qquad \overline{v^2} = 1.0\,U_\tau^2, \qquad \overline{w^2} = 2.3\,U_\tau^2$$

$$\overline{uv} = -U_\tau^2 + y\,\frac{d\bar{P}}{dx}, \qquad \epsilon = -\,\overline{uv}\,\frac{dU}{dy} \tag{24}$$

where U_τ is the friction velocity, and x and y denote, respectively, the distances measured along and normal to the surface. It needs to be mentioned here that, in the present wall-function approach, the friction velocity is modified as $U_\tau = \mathrm{sign}(\tau_w)\,(|\tau_w|/\rho)^{1/2}$, where τ_w is the wall shear stress, as was done in Ghose and Kline[18] to treat the region of reversed flow.

Results and Discussion

To evaluate the performance of the present curvature-dependent Reynolds-stress model, calculation has been performed for the flow about a spheroid of axis ratio 6:1 at $Re = 2.75 \times 10^6$. Here, the Reynolds number is based on the freestream velocity U_o and the body length L. A 60×30 grid is fitted over the physical domain $0.4 \le X/L \le 13.8$ and $R_s/L \le R/L \le 1.0$, where X is the distance measured along the axis from the nose, R the radial distance from the axis, and subscript s denotes the body surface. The wall-function approach permits us to use a relatively coarse grid near the wall, with the first grid point located at $y^+ \simeq 30$. Calculation was also performed with a 40×20 grid to check the grid dependency of the solution. The results were in close agreement with each other and confirm that the 60×30 grid is fine enough to resolve the flowfield.

Figure 2 shows the pressure distribution on the surface and along the centerline of the wake. The calculations by the present CRSM with and without the curvature effects are compared with the experimental data of Chevray.[9] The earlier result of Chen and Patel,[10] who used the two-layer k-ϵ model, is also compared in the figure. The present result is in good agreement with the experimental data, especially the pressure peak, while the prediction of Chen and Patel overestimates the peak value substantially. The pressure rise in the immediate vicinity of the tail is associated with the large longitudinal and transverse curvatures.

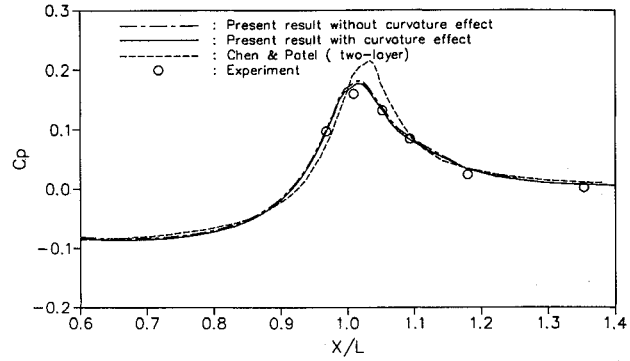

Fig. 2 Pressure distribution over the spheroid surface and along the wake centerline.

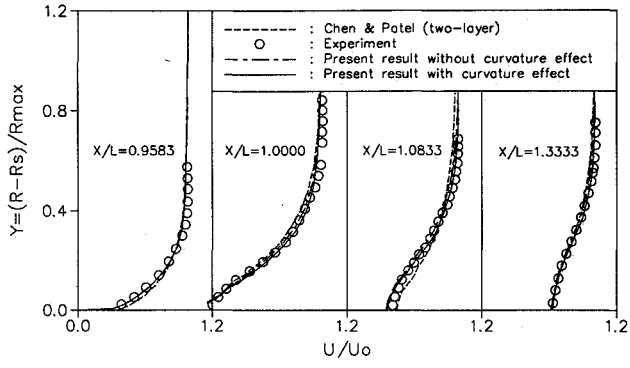

Fig. 3 Mean velocity profiles.

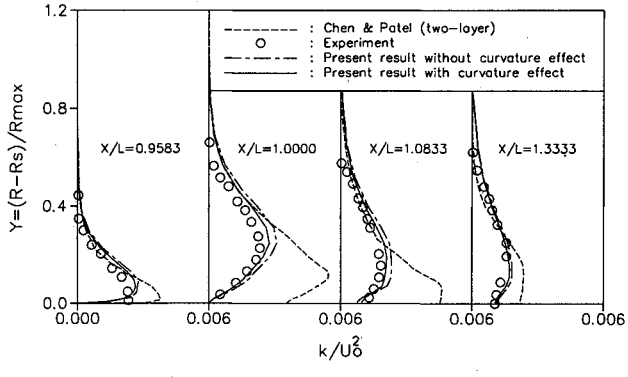

Fig. 4 Turbulent kinetic energy profiles.

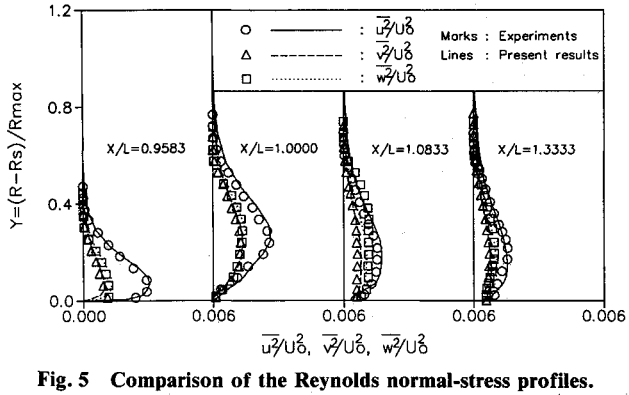

Fig. 5 Comparison of the Reynolds normal-stress profiles.

Figure 3 shows the streamwise mean velocity distributions at various locations: the location $X/L = 0.958$ is upstream of the separation point, $X/L = 1.0$ falls within the separation bubble, $X/L = 1.083$ is just after the closing of the separation bubble, and $X/L = 1.333$ is in the wake. Here, R_{max} denotes the maximum body radius. It can be seen that the present predictions are in better agreement with the data than those of Chen and Patel.[10] The improvement can be attributed to the

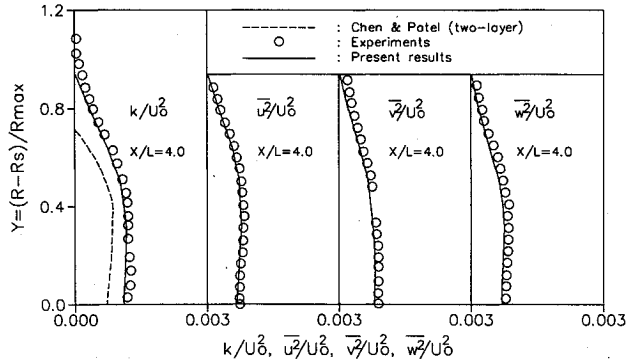

Fig. 6 Distributions of turbulent kinetic energy and Reynolds normal stresses far downstream in the wake.

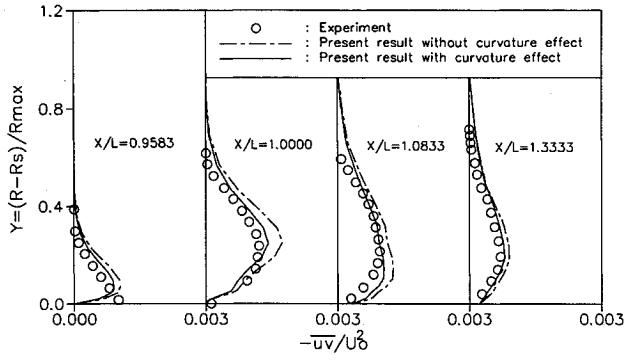

Fig. 7 Reynolds shear-stress profiles.

length-scale adjustment by the present model according to the convexity or concavity of streamline curvature near the separation bubble. In the outer part of the separated shear layer above the separation bubble, the length scale is shortened by the increased dissipation rate, caused by a reduction in $C'_{\epsilon 2}$ by the convexly curved streamlines. However, in the wake, the length scale is slightly increased due to the opposite mechanism and increase of $C'_{\epsilon 2}$. When the curvature correction is removed from the present model, the results fall in between the two predictions.

The turbulent kinetic-energy distributions at the same streamwise locations are shown in Fig. 4. Here, attention is drawn to the predictions by the present model with and without curvature effects. As the streamlines near $X/L = 1.0$ are highly convex, the turbulent kinetic energy is expected to be reduced. This trend is correctly predicted by the curvature-dependent model. On the other hand, it is observed that both the Reynolds-stress model without curvature effects and the k-ϵ model overpredict the turbulent kinetic energy. This is a consequence of the fact that these models do not take account of the stabilization effect of convex streamline curvature. The discrepancy noted in the result of the k-ϵ model may also be due to the anisotropy of the turbulence (see Fig. 5).

Figure 5 shows the distributions of the normal stresses, $\overline{u^2}$, $\overline{v^2}$, and $\overline{w^2}$. It reveals that the turbulence is highly anisotropic and that the present results are in excellent agreement with the experimental data. Figure 6 presents the turbulent kinetic energy and the normal stresses at a station farther downstream in the wake, $X/L = 4.0$. It is interesting to observe from Figs. 5 and 6 that the streamwise turbulence intensity $\overline{u^2}$, which is highest in $X/L \leq 1.0$, decreases rapidly to attain near equipartitioning of energy among the three components in the wake region and that it is correctly predicted by the present model. The shear stress $-\overline{uv}$ is compared in Fig. 7. Here again the improvement due to the curvature correction in the turbulence model is clearly observed.

Conclusions

A curvature-dependent Reynolds stress model (CRSM) has been applied to predict the turbulent flow over a mildly curved axisymmetric body. This model adjusts the turbulence length scale according to the convexity or concavity of the streamlines because the time scales of the third-order diffusive transport terms and the destruction term in the dissipation-rate equation are made functions of the ratio between the curvature and the velocity time scales. It has been shown that such a modification yields much better predictions of the streamwise mean velocity and the turbulent kinetic energy than the k-ϵ turbulence model. Also, the Reynolds normal stresses, which exhibit high degree of anisotropy in the neighborhood of the tail, are well predicted by the present model.

Acknowledgment

The authors would like to express their deep appreciation to V. C. Patel for his valuable comments and suggestions that have led to an improvement of the paper.

References

[1]Kline, S. J., Cantwell, B. J., and Lilley, G. M. (eds.) *Proceedings of the 1980-81 AFOSR-HTTM-Stanford Conference on Complex Turbulent Flows,* Vols. 1-3, Stanford Univ., Stanford, CA, 1982.

[2]Smits, A. J., Young, S. T. B., and Bradshaw, P., "The Effects of Short Regions of High Surface Curvature on Turbulent Boundary Layers," *Journal of Fluid Mechanics*, Vol. 94, 1979, pp. 209-242.

[3]Amano, R. S., and Goel, P., "Computations of Turbulent Flow Beyond Backward Facing Steps Using Reynolds Stress Closure," *AIAA Journal*, Vol. 23, No. 9, 1985, pp. 1356-1361.

[4]Irwin, H. P. A. H., and Smith, P. A., "Prediction of Effects of Streamline Curvature on Turbulence," *Physics of Fluids*, Vol. 18, No. 6, 1975, pp. 624-630.

[5]Militzer, J., Nicoll, W. B., and Alpay, S. A., "Some Observations on the Numerical Calculation of the Recirculation Region of Twin Parallel Symmetric Jet Flow," *Proceedings of the Symposium on Turbulent Shear Flows,* Pennsylvania State Univ., University Park, PA, 1977, pp. 18.11-18.18.

[6]Leschziner, M. A., and Rodi, W., "Calculation of Annular and Twin Parallel Jets Using Various Discretization Schemes and Turbulence Model Variations," *Journal of Fluids Engineering*, Vol. 103, 1981, pp. 352-360.

[7]Launder, B. E., Priddin, C. H., and Sharma, B. S., "The Calculation of Turbulent Boundary Layers on Spinning and Curved Surfaces," *Journal of Fluids Engineering*, Vol. 99, March 1977, pp. 231-239.

[8]Park, S. W., and Chung, M. K., "Development of Curvature-Dependent Two-Equation Model for Prediction of Two-Dimensional Recirculating Flows," *AIAA Journal*, Vol. 27, March 1989, pp. 340-344.

[9]Chevray, R., "The Turbulent Wake of a Body of Revolution," *Journal of Basic Engineering*, Vol. 9, June 1968, pp. 275-284.

[10]Chen, H. C., and Patel, V. C., "The Wake of an Axisymmetric Body with and without Tail Separation," *Sixth Symposium on Turbulent Shear Flows*, Toulouse, France, 7-9 Sept., 1987.

[11]Tennekes, T., and Lumley, J. L., *A First Course in Turbulence,* MIT Press, Cambridge, MA, 1972, Chap. 2.

[12]Launder, B. E., Reece, G. J., and Rodi, W., "Progress in the Development of a Reynolds-Stress Turbulence Closure," *Journal of Fluid Mechanics*, Vol. 68, Pt. 3, April 1975, pp. 538-566.

[13]Hanjalic, K., and Launder, B. E., "Contribution Towards a Reynolds-Stress Closure for Low-Reynolds Number Turbulence," *Journal of Fluid Mechanics*, Vol. 74, Pt. 4, 1976, pp. 593-610.

[14]Nobuyuki, S., "A Reynolds-Stress Model for Near Wall and Low-Reynolds Number Regions," *Journal of Fluids Engineering*, Vol. 110, March 1988, pp. 38-44.

[15]Chung, M. K., Park, S. W., and Kim, K. C., "Curvature Effects on Third-Order Velocity Correlation and Its Model Representation," *Physics of Fluids*, Vol. 30, April 1987, pp. 609-638.

[16]Chen, H. C., and Patel, V. C., "Calculation of Trailing-Edge, Stern, and Wake Flows by a Time-Marching Solution of the Partially Parabolic Equation," Iowa Inst. of Hydraulic Research, Univ. of Iowa, Iowa City, IA, IIHR Rept. 285, April 1985.

[17]Chang, K. C., and Patel, V. C., "Calculation of Three-Dimensional Boundary Layers on Ship Forms," Iowa Inst. of Hydraulic Research, Univ. of Iowa, Iowa City, IA, IIHR Rept. 178, June 1975.

[18]Ghose, S., and Kline, S. J., "The Computation of Optimum Pressure Recovery in Two-Dimensional Diffusers," *Journal of Fluids Engineering*, Vol. 100, Dec. 1978, pp. 419-426.